

A Drought Dataset Based on a Composite Index for the Sahelian Climate Zone of Niger

Issa Garba ¹, Zakari Seybou Abdourahamane ^{1,*} and Alisher Mirzabaev ² 

¹ Agrhymet Regional Centre, Niamey P.O. Box 11011, Niger

² Center for Development Research, University of Bonn, 53113 Bonn, Germany

* Correspondence: abdourahamane.zakari@cilss.int

Abstract: Agricultural drought monitoring in Niger is relevant for the implementation of effective early warning systems and for improving climate change adaptation strategies. However, the scarcity of in situ data hampers an efficient analysis of drought in the country. The present dataset was created for agricultural drought characterization in the Sahelian climate zone of Niger. The dataset comprises the three-month scale and monthly time series of a composite drought index (CDI) and their corresponding drought classes at a spatial resolution of 1 km² for the period 2000–2020. The CDI was generated from remote sensing data, namely CHIRPS (Climate Hazards Group InfraRed Precipitation with Stations), normalized difference vegetation index (NDVI) and land surface temperature (LST) from MODIS (Moderate Resolution Imaging Spectroradiometer). A weighing technique combining entropy and Euclidian distance was applied in the CDI derivation. From the present dataset, the extraction of the CDI time series can be performed for any location of the study area using its geographic coordinates. Therefore, seasonal drought characteristics, such as onset, end, duration, severity and frequency can be computed from the CDI time series using the theory of runs. The availability of the present dataset is relevant for the socio-economic assessment of drought impacts at small spatial scales, such as district and household level. This dataset is also important for the assessment of drought characteristics in remote areas or areas inaccessible due to civil insecurity in the country as it was entirely generated from remote sensing data. Finally, by including temperature data, the dataset enables drought modelling under global warming.

Keywords: CHIRPS; drought; LST; MODIS; NDVI; Sahel



Citation: Garba, I.; Abdourahamane, Z.S.; Mirzabaev, A. A Drought Dataset Based on a Composite Index for the Sahelian Climate Zone of Niger. *Data* **2023**, *8*, 28. <https://doi.org/10.3390/data8020028>

Academic Editor: Vladimir Sreckovic

Received: 8 November 2022

Revised: 12 December 2022

Accepted: 13 December 2022

Published: 28 January 2023



Copyright: © 2023 by the authors. Licensee MDPI, Basel, Switzerland. This article is an open access article distributed under the terms and conditions of the Creative Commons Attribution (CC BY) license (<https://creativecommons.org/licenses/by/4.0/>).

1. Introduction

Drought is one of the most complex and costliest natural hazards. It is difficult to accurately identify its onset and end, as it generally starts slowly and gradually. The impacts of drought are context-dependent, they are mostly diffuse, both direct and indirect, short-term and long-term [1].

According to the International Disaster Database [2], over 1.1 billion people were affected by droughts, globally, between 1994 and 2013. In this period, the African continent registered about 131 droughts, being the most affected continent [3]. In the Sahel region, drought remains a key driver of food insecurity. The Sahelian droughts of the 1970s and 1980s is clear evidence of how droughts could affect livestock and crop productivity, causing food insecurity and mass migration [4,5]. These unprecedented droughts also contributed to land degradation and increasing desertification. Due to its socioeconomic context, the Sahel region is considered one of the most vulnerable regions to climate change [6].

In the Sahel region, drought is often combined with locust infestation, conflicts and political instability, causing emergency situations. For example, in 2009, drought in Niger was combined with locust infestation, leading to approximately 805 million USD of losses, which corresponds to 30% of the GDP of the country [7]. Moreover, the 2010 drought in the country affected the food security of about 40% of the population [7].

To effectively respond to drought, a comprehensive assessment of its socioeconomic and environmental impacts is required. However, to understand drought impacts its spatiotemporal characterization is necessary. This is traditionally achieved by using drought indicators or indices. There are over 100 different indices used to measure drought [8]. The computation of these indices requires historical hydroclimatic data collected from ground stations, which are generally scarce in the Sahel region. Furthermore, the use of drought indices based only on one input variable, such as the precipitation anomalies, quantiles or the standardized precipitation index (SPI) [9] may fail to assess the joined characteristics of different types of droughts (e.g., meteorological, agricultural and hydrological drought).

In recent years, earth observation data have been used as an alternative to in situ measurement of hydroclimatic and land data to compute drought indices [10–13]. Additionally, the use of composite drought indices (CDI) has enabled the characterization of combined droughts effects [10,14,15].

The present data article aims to generate a database of drought characteristics based on a composite index derived from remotely sensed data, namely precipitation, temperature and vegetation at 1 km² resolution for Niger.

The availability of drought data, at 1 km² resolution, based entirely on remote sensing data is relevant for drought characterization and impacts assessment at small spatial scale in the country.

2. Data and Methods

2.1. Study Area

Niger is a country located in West Africa at the southern edge of the hyper arid Sahara Desert. The economy of the country is mainly based on rainfed agriculture, livestock raising and mining. Agriculture is practiced in the Sahelian zone (Figure 1) of the country which is characterised by a semi-arid climate. The Sahel region, in general, is recognised as one of the regions that is highly vulnerable to the adverse effects of climate change. In the Sahelian climate zone, the rainy season is short (Jun to September) with annual rainfall amount of about 350 to 850 from north to south. Rainfall data in the country is recorded by a network of 15 climate stations and about 200 rain gages for an area of 1.2 million km². Currently, a high-density network of uniformly distributed rain gauges is scarce and many of the climate stations are out of service; therefore, large parts of the country lack rainfall information. Mean daily temperatures in the country increase from south to north between 9 °C and 45 °C depending on the season. Recurrent droughts are among the main factors that slow down the economic development of the country.

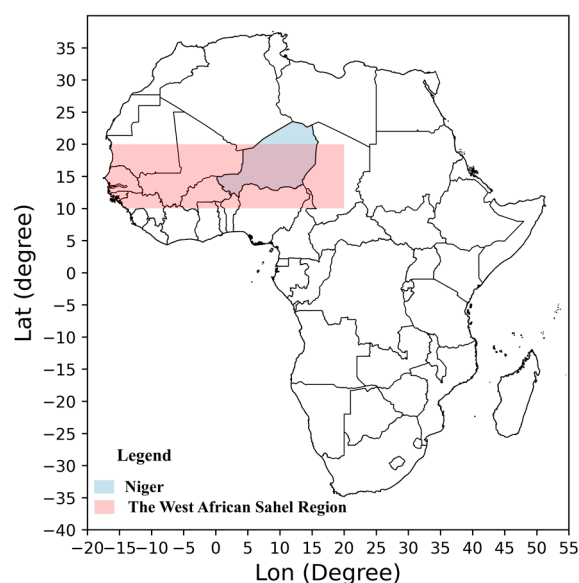


Figure 1. Study Area.

Several studies have linked the 1970s and 1980s droughts in the Sahel region to large-scale climate indices, such as El Niño-Southern Oscillation (ENSO) or sea surface temperature of the Tropical Atlantic Ocean [16–19]. However, further research is needed to investigate the dynamic of the link between drought in this region and large-scale climate indices, such as ENSO.

2.2. Input Data Description

Remote sensing data of rainfall, temperature and vegetation were used to compute the CDI for agricultural drought characterization in Niger. These input variables are, respectively, the Climate Hazards Group InfraRed Precipitation with Stations (CHIRPS) [20], the normalized difference vegetation index (NDVI) [21,22] and the land surface temperature (LST) [23] from MODIS (Moderate Resolution Imaging Spectroradiometer) launched by the National Aeronautic and Space Administration (NASA, Washington, DC, USA). The MODIS instruments were built by Santa Barbara Remote Sensing (Santa Barbara, California). All the input variables cover the period 2000–2020. Figures 2–4 show the average seasonal (July–September) CHIRPS rainfall amount, the mean seasonal NDVI and the mean daytime LST over the period 2000–2020, respectively, for the Sahelian climate zone of Niger.

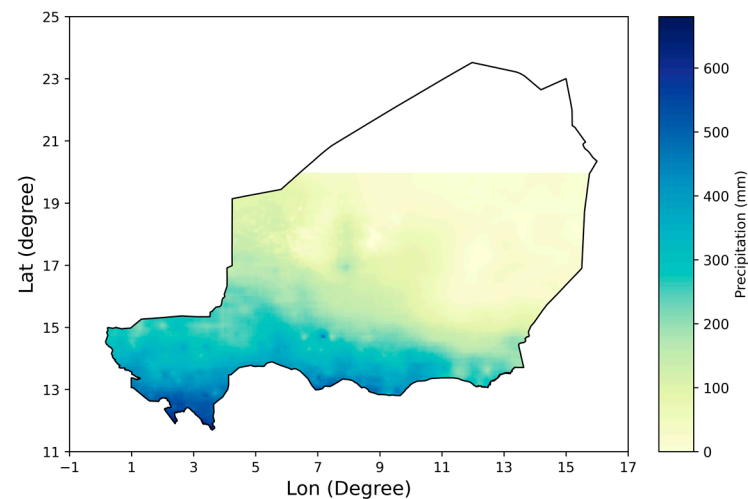


Figure 2. Long-term (2000–2020) mean of the accumulated seasonal CHIRPS rainfall.

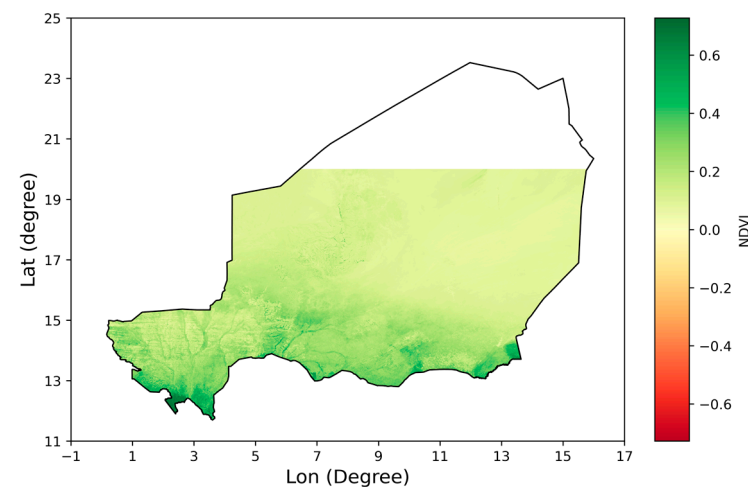


Figure 3. Long-term (2000–2020) mean of the seasonal NDVI.

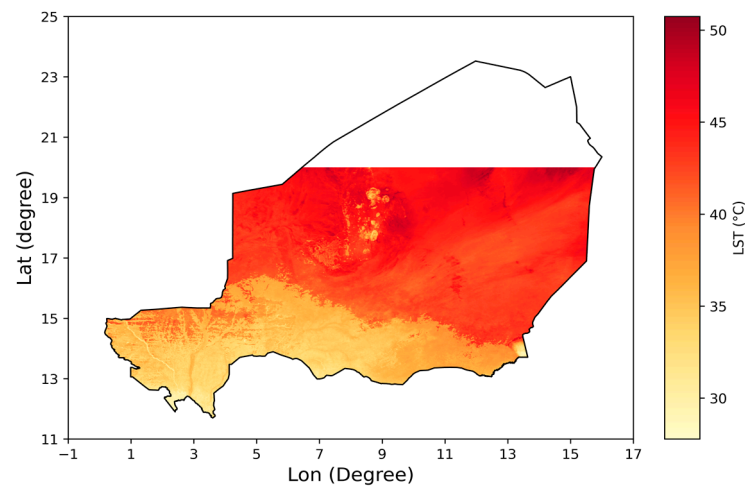


Figure 4. Long-term (2000–2020) mean of the daytime LST.

The CHIRPS rainfall products are bias-corrected using ground observation data. According to [24], the CHIRPS data provide reasonable rainfall estimates compared to other satellite products over the Sahel region. The monthly CHIRPS rainfall data were retrieved from the University of California website (<https://chc.ucsb.edu/data/chirps>, accessed on 15 April 2022). The data were spatially resampled from $0.05^\circ \times 0.05^\circ$ Longitude/Latitude to $1 \text{ km} \times 1 \text{ km}$ by conserving the rainfall amount in the original grid box.

The main source of uncertainty in the MODIS NDVI, used herein, is the presence of aerosol that may impact its accuracy mainly over arid bright surfaces [22]. The overall accuracy of the MODIS vegetation indices is within ± 0.025 in optimal observation conditions—such as clear, no sub-pixel cloud or low aerosol [22]. The MODIS NDVI has been successfully used by [25] to assess vegetation fluctuations in the Sahel region.

As for the MODIS LST at 1 km^2 resolution, several studies—based on initial validation or uncertainty simulations—have shown its accuracy over all land cover types regardless to the atmospheric conditions [26–28].

The NDVI and LST data were retrieved from the USGS (United States Geological Survey) website (<https://lpdaac.usgs.gov/tools/appeears/>, accessed on 18 April 2022) using the AppEEARS (Application for Extracting and Exploring Analysis Ready Samples) tool. In this tool, the Sahel climate zone of Niger was delineated, and the temporal coverage was specified.

2.3. Development of the Composite Drought Index

Prior to the CDI computation, the input variables were grouped into two categories. The computation was carried out separately for the monthly CDI and the three-month scale CDI, hereinafter CDI-3. The first category, A, contains the LST data as it is proportional to drought occurrence, and the second category, B, contains the precipitation and NDVI data as they contribute to wet spells.

The first step of the CDI computation consisted of the determination of the entropy weights. To attribute objective weights, the input variables were normalised using Equation (1) as follows:

$$r_{ki} = x_{ki} / \sum_{i=1}^m x_{ki} \quad (1)$$

r_{ki} is the normalised value and x_{ki} corresponds to the value of the k th input variable with time index i ($i = 1, 2, \dots, m$).

After the data normalisation, the entropy measure, e_k , of each variable was determined as follows:

$$e_k = \frac{-\sum_{i=1}^m r_{ki} \ln(r_{ki})}{\ln(m)} \quad (2)$$

For $r_{ik} = 0$, Equation (2) becomes $e_k = \frac{r_{ki}}{\sum_{i=1}^m r_{ki}}$.

In the next step, the degree of diversification of each input was computed by applying the following expression:

$$D_k = 1 - e_k \quad (3)$$

Then, the entropy weight of each input variable was obtained using Equation (4):

$$Ew_k = \frac{D_k}{\sum_{j=1}^k D_k} \quad (4)$$

Ew_k is the entropy weight which ranges from 0 to 1 so that $\sum_{j=1}^k D_k = 1$.

Once the entropy weight is computed, the next step consists of determining the maximum driest condition (MDC) and the maximum wettest condition (MWC). For the variables in A category (LST), MDC and MWC correspond to the maximum and minimum values of the normalised series (r_{ki}), respectively. As for the precipitation and NDVI, belonging to B category, MDC and MWC correspond to the minimum and maximum values of r_{ki} , respectively.

$$MDC_k = \{\max(r_{ki}), k \in A; \min(r_{ki}), k \in B\} \quad (5)$$

$$MWC_k = \{\min(r_{ki}), k \in A; \max(r_{ki}), k \in B\} \quad (6)$$

The weighted Euclidian distance between the present condition (PC), which is the value of the normalised indicator at time t_i , $PC = (r_{1i}, r_{2i}, \dots, r_{ki})$, and the MDC and MWC were computed using Equations (7) and (8), respectively:

$$S_i^- = \sqrt{\sum_{k=1}^n Ew_k [r_{ki} - MDC_k]^2} \quad (7)$$

$$S_i^+ = \sqrt{\sum_{k=1}^n Ew_k [r_{ki} - MWC_k]^2} \quad (8)$$

S_i^- is the weighted Euclidian distance between PC and MDC and S_i^+ is the weighted Euclidian distance between PC and MWC.

Finally, the time series of the CDI is computed using Equation (9) following [29]:

$$CDI_i = \frac{S_i^-}{S_i^- + S_i^+} \quad (9)$$

The CDI values ranges between 0 and 1. The computation of the CDI was carried out in Python software [30].

3. Data Description

The generated dataset was published in a Mendeley repository, and contains:

A NetCDF file named "cdi_3.nc.zip" of the CDI-3 time series and the corresponding drought classes from 2000 to 2020.

A folder named "Input data to the CDI-3" containing each of the input variables (CHIRPS, NDVI and LST) to the CDI-3 in NetCDF format for 2000–2020.

A folder named "Monthly CDI" containing three subfolders of the monthly CDI and the inputs variables for July, August and September, and

Map files of Niger in ESRI shapefile format.

These data are available in a Mendeley repository under the name "Dataset of a composite drought index based on remote sensing data for Niger" at the following address: <https://data.mendeley.com/datasets/47ydz8v6nd>, accessed on 20 September 2022.

Overall, the dataset has a spatial resolution of 1 km² and covers the territory of Niger, except the Sahara Desert, for the period 2000–2020. For instance, a description of the variables, coordinates and dimensions of the CDI-3 is given in Figure 5. In this figure, a screenshot of the data read in Python version 3.8.2 [30] using the “xarray” library is shown.

```

► Dimensions:      (lat: 994, lon: 1874, year: 21)
▼ Coordinates:
lat              (lat)          float64  19.97 19.96 19.95 ... 11.7 11.7
array([19.970833, 19.9625 , 19.954167, ..., 11.7125 , 11.704167, 11.695833])
lon              (lon)          float64  0.1625 0.1708 ... 15.76 15.77
array([ 0.1625 ,  0.170833,  0.179167, ..., 15.754167, 15.7625 , 15.770833])
year             (year)         int64   2000 2001 2002 ... 2018 2019 2020
array([2000, 2001, 2002, 2003, 2004, 2005, 2006, 2007, 2008, 2009, 2010, 2011,
       2012, 2013, 2014, 2015, 2016, 2017, 2018, 2019, 2020])
spatial_ref      ()             int64   ...
▼ Data variables:
CDI              (lat, lon, year) float64 ...
[39117876 values with dtype=float64]
drought_class    (lat, lon, year) object ...
[39117876 values with dtype=object]
▼ Attributes:
grid_mapping :   spatial_ref

```

Figure 5. Screenshot of the NetCDF file of the drought data read in Python software.

Additionally, drought maps can be generated for each year of the study period (2000–2020) and for the months of July, August and September, as explained in the steps for reproducing the data in the data source (<https://data.mendeley.com/datasets/47ydz8v6nd>, accessed 20 September 2022). For instance, Figure 6 shows the seasonal drought intensity of the 2000 based the CDI-3 series.

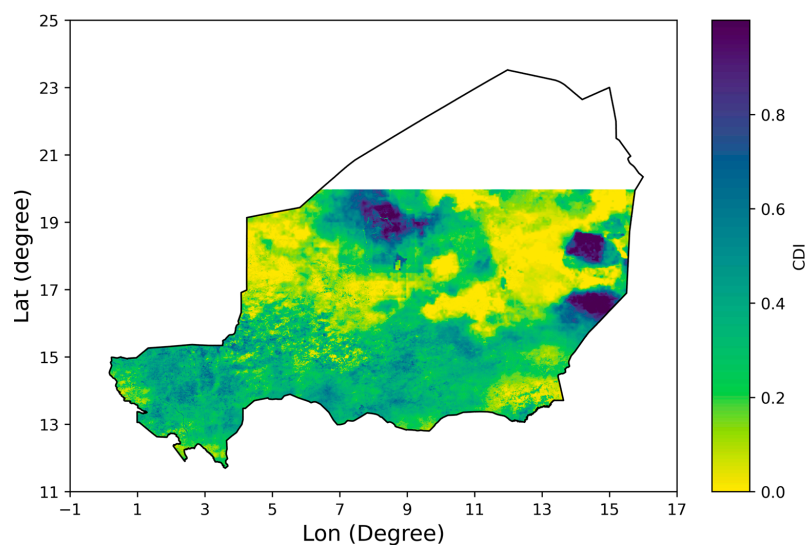


Figure 6. Drought map of 2000 based on CDI-3 for Niger.

To understand the map of Figure 6, the drought classification based on the CDI values is needed (Table 1).

Table 1. Drought classes based on the CDI values following [10,29].

CDI Interval	Classification
<0.1	Extreme Drought
0.1–0.2	Severe Drought
0.2–0.3	Moderate Drought
0.3–0.4	Mild Drought
0.4–0.5	Near Normal
>0.5	Above Normal

From Table 1, drought occurs when the CDI value is below 0.4.

Moreover, from the drought dataset, drought intensities can be extracted using geographic coordinates for a given location or an area of interest. Thus, from the CDI time series, drought characteristics, such as onset, end, duration, spatial spread and frequency can be computed following [10].

The python codes to exploit the data are given in the “Steps to reproduce” in the Mendeley repository. In these steps, the algorithms for the extraction of the CDI times series at a given location or for a specific area are explained. For instance, Table 2 presents the CDI-3 times series and drought classes at a location with latitude of 13.5 degree and longitude of 3.00 degree.

Table 2. CDI and drought classes at latitude = 13.5 degree and longitude = 3.00 degree.

Year	CDI-3	Drought Class
2000	0.313	Mild drought
2001	0.478	Near normal
2002	0.403	Near normal
2003	0.368	Mild drought
2004	0.368	Mild drought
2005	0.511	Above normal
2006	0.642	Above normal
2007	0.528	Above normal
2008	0.409	Near normal
2009	0.454	Near normal
2010	0.442	Near normal
2011	0.000	Extreme drought
2012	0.601	Above normal
2013	0.604	Above normal
2014	0.261	Moderate drought
2015	0.722	Above normal
2016	0.350	Mild drought
2017	0.447	Near normal
2018	0.590	Above normal
2019	0.447	Near normal
2020	0.780	Above normal

The drought characteristics derived from the CDI-3 time series of Table 2 are shown in Table 3.

Table 3. Drought characteristics at latitude = 13.5 degree and longitude = 3.00 degree.

Event Order	Onset	End	Duration (Year)	Severity	Average Return Period (Year)
1	2000	2000	1	0.087	3.33
2	2003	2004	2	0.064	
3	2011	2011	1	0.400	
4	2014	2014	1	0.139	

As for the quality control, reference drought indices, mainly the standardised precipitation index (SPI) and the standardised precipitation evapotranspiration index (SPEI) computed from station data were used to validate the CDI. A good correlation coefficient was found between the CDI-3 and these reference drought indices (Table 4).

Table 4. Pearson correlation coefficients between the CDI-3 and station-based references drought indices.

Station Name	Longitude	Latitude	Correlation Coefficients	
			CDI-SPI	CDI-SPEI
Niamey-Aero	2.17	13.48	0.64	0.7
Tahoua	5.30	14.90	0.74	0.78
Diffa	12.62	13.42	0.73	0.77
Zinder	8.98	13.78	0.66	0.67

Additionally, the ability of the CDI to monitor agricultural drought was checked by performing a correlation analysis between the CDI-3 time series and production data of millet and sorghum from the FAOSTAT database [31]. Pearson correlation coefficients of 0.58 and 0.57 were found between the areal mean of the CDI-3 and production data of millet and sorghum, respectively.

The comparison between the CDI, SPI and SPEI drought classes (Figure 7) showed that the CDI agrees with ground observation-based indices; however, the CDI performs better in terms of sensitivity as it detects more drought classes.

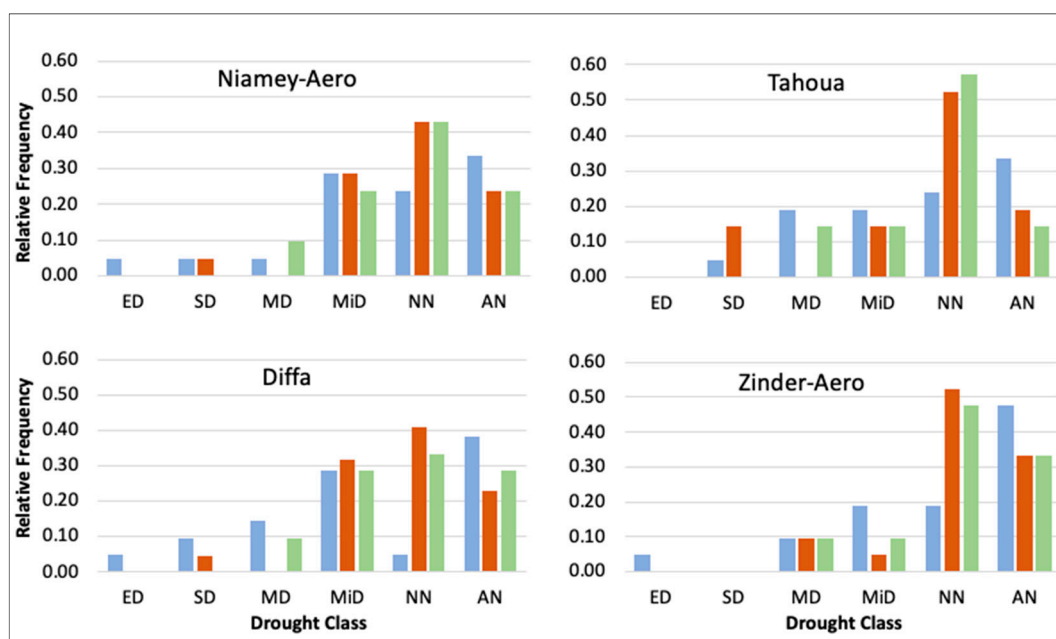


Figure 7. Comparison of drought classes between the CDI-3 and ground observation-based SPI-3 and SPEI-3 at four stations.

Furthermore, the availability of the CDI at monthly time scale enables the assessment of seasonal changes in drought patterns.

4. Conclusions

The present dataset, which was generated entirely from remote sensing data, is an alternative for ground-observation-based drought indices for understanding drought dynamics in Niger. With a spatial resolution of 1 km², this dataset is a useful tool for assessing drought characteristics and its impact at rural district and household levels. By including precipitation, vegetation and temperature data in the computation of the composite drought index (CDI), the combined impacts of meteorological and agricultural droughts can be assessed with more accuracy. The current dataset also enables the assessment of drought dynamics under a context of climate change as it includes temperature data. All the input data to the computation of the CDI are freely available on many online platforms of Earth observation data. Moreover, the tool used for the computation, namely the Python software, is open source. Therefore, the proposed methodology can be reproduced and further research on this topic can be carried out without any difficulty. Finally, the dataset and its input variables are freely accessible on a Mendeley repository.

Author Contributions: Conceptualization, I.G.; methodology, I.G. and Z.S.A.; software, Z.S.A.; validation I.G., Z.S.A. and A.M; formal analysis, I.G., Z.S.A. and A.M; investigation, Z.S.A.; data curation Z.S.A. and I.G; writing—original draft preparation, I.G., Z.S.A. and A.M; writing—review and editing, I.G., Z.S.A. and A.M; supervision, A.M. and I.G.; project administration, I.G. and A.M.; funding acquisition, A.M. All authors have read and agreed to the published version of the manuscript.

Funding: This research was funded by the Program of Accompanying Research on Agricultural Innovation (PARI) [2014.0690.9], supported by the German Federal Ministry for Economic Cooperation and Development (BMZ).

Institutional Review Board Statement: Not applicable.

Informed Consent Statement: Not applicable.

Data Availability Statement: Link to the dataset: <https://data.mendeley.com/datasets/47ydz8v6nd>.

Acknowledgments: This study was developed in the context of the Program of Accompanying Research on Agricultural Innovation (PARI) (2014.0690.9), supported by the German Federal Ministry for Economic Cooperation and Development (BMZ).

Conflicts of Interest: The authors declare that they have no known competing financial interest or personal relationships that could have appeared to influence the work and data reported in this article.

References

1. Wilhite, D.; Pulwarty, R.S. (Eds.) *Drought and Water Crises: Integrating Science, Management, and Policy*; CRC Press: Boca Raton, FL, USA, 2017.
2. Guha-Sapir, D.; Below, R.; Hoyois, P. EM-DAT: International Disaster Database. Brussels, Belgium: Université Catholique de Louvain. 2014. Available online: www.emdat.be (accessed on 20 May 2022).
3. CRED. *Human Cost of Natural Disasters: A Global Perspective*; CRED and UNISDR: Brussels, Belgium, 2015; p. 59.
4. Hein, L.; De Ridder, N. Desertification in the Sahel: A reinterpretation. *Glob. Change Biol.* **2006**, *12*, 751–758. [[CrossRef](#)]
5. Molua, E.L. *The Economic Impact of Climate Change on Agriculture in Cameroon*; World Bank Policy Research Working Paper 2007; World Bank: Washington, DC, USA, 2007; Volume 4364.
6. Abdourahamane, Z.S.; Acar, R.; Serkan, Ş. Wavelet–copula-based mutual information for rainfall forecasting applications. *Hydrol. Process.* **2019**, *33*, 1127–1142. [[CrossRef](#)]
7. World Bank Group. Republic of Niger Priorities for Ending Poverty and Boosting Shared Prosperity: Systematic Country Diagnostic. World Bank, Washington, DC, USA, 2017. World Bank, License: CC BY 3.0 IGO. Available online: <https://openknowledge.worldbank.org/handle/10986/28994> (accessed on 16 June 2022).
8. Zargar, A.; Sadiq, R.; Naser, B.; Khan, F.I. A review of drought indices. *Environ. Rev.* **2011**, *19*, 333–349. [[CrossRef](#)]
9. McKee, T.B.; Doesken, N.J.; Kleist, J. The relationship of drought frequency and duration to time scales. In Proceedings of the 8th Conference on Applied Climatology, Anaheim, CA, USA, 17–22 January 1993; pp. 179–183.

10. Abdourahamane, Z.S.; Garba, I.; Boukary, A.G.; Mirzabaev, A. Spatiotemporal characterization of agricultural drought in the Sahel region using a composite drought index. *J. Arid Environ.* **2022**, *204*, 104789. [[CrossRef](#)]
11. Liu, Q.; Zhang, S.; Zhang, H.; Bai, Y.; Zhang, J. Monitoring drought using composite drought indices based on remote sensing. *Sci. Total Environ.* **2020**, *711*, 134585. [[CrossRef](#)] [[PubMed](#)]
12. Anderson, M.C.; Hain, C.; Wardlow, B.; Pimstein, A.; Mecikalski, J.R.; Kustas, W.P. Evaluation of drought indices based on thermal remote sensing of evapotranspiration over the continental United States. *J. Clim.* **2011**, *24*, 2025–2044. [[CrossRef](#)]
13. Vicente-Serrano, S.M.; Cabello, D.; Tomás-Burguera, M.; Martín-Hernández, N.; Beguería, S.; Azorin-Molina, C.; El Kenawy, A. Drought variability and land degradation in semiarid regions: Assessment using remote sensing data and drought indices (1982–2011). *Remote Sens.* **2015**, *7*, 4391–4423. [[CrossRef](#)]
14. Balint, Z.; Mutua, F.; Muchiri, P.; Omuto, C.T. Monitoring drought with the combined drought index in Kenya. In *Developments in Earth Surface Processes*; Elsevier: Amsterdam, The Netherlands, 2013; Volume 16, pp. 341–356.
15. Al Adaileh, H.; Al Qinna, M.; Barta, K.; Al-Karablieh, E.; Rakonczai, J.; Alobeiaat, A. A drought adaptation management system for groundwater resources based on combined drought index and vulnerability analysis. *Earth Syst. Environ.* **2019**, *3*, 445–461. [[CrossRef](#)]
16. Folland, C.K.; Owen, J.; Ward, M.N.; Colman, A. Prediction of seasonal rainfall in the Sahel region using empirical and dynamical methods. *J. Forecast* **1991**, *10*, 21–56. [[CrossRef](#)]
17. Janicot, S.; Moron, V.; Fontaine, B. Sahel droughts and ENSO dynamics. *Geophys. Res. Lett.* **1996**, *23*, 515–518. [[CrossRef](#)]
18. Joly, M.; Voldoire, A.; Douville, H.; Terray, P.; Royer, J.-F. African monsoon teleconnections with tropical SSTs: Validation and evolution in a set of IPCC4 simulations. *Clim Dyn.* **2007**, *29*, 1–20. [[CrossRef](#)]
19. Giannini, A.; Michel, M.; Verstraete, M. A climate model-based re- view of drought in the Sahel: Desertification, the re-greening and climate change. *Glob. Planet Chang.* **2008**, *64*, 119–128. [[CrossRef](#)]
20. Funk, C.C.; Peterson, P.J.; Landsfeld, M.F.; Pedreros, D.H.; Verdin, J.P.; Rowland, J.D.; Romero, B.E.; Husak, G.J.; Michaelsen, J.C.; Verdin, A.P. A quasi-global precipitation time series for drought monitoring. *US Geol. Surv. Data Ser.* **2014**, *832*, 1–12.
21. Rouse, J.W., Jr.; Haas, R.H.; Schell, J.A.; Deering, D.W. *Monitoring Vegetation Systems in the Great Plains with ERTS*; NASA Special Publication: Washington, DC, USA, 1974; Volume 351, p. 309.
22. Didan, K. MOD13A3 MODIS/Terra vegetation Indices Monthly L3 Global 1km SIN Grid V006 [Data set]. NASA EOSDIS Land Processes DAAC 2015. Available online: <https://doi.org/10.5067/MODIS/MOD13A3.006> (accessed on 15 April 2021).
23. Wan, Z. New refinements and validation of the collection-6 MODIS land-surface temperature/emissivity product. *Remote Sens. Environ.* **2014**, *140*, 36–45. [[CrossRef](#)]
24. Gbode, I.E.; Intsiful, J.D.; Akisanola, A.A.; Abolude, A.T.; Ogunjobi, K.O. Uncertainties in daily rainfall over West Africa: Assessment of gridded products and station gauges. In *Climate Impacts on Extreme Weather*; Elsevier: Amsterdam, The Netherlands, 2022; pp. 65–82.
25. Brandt, M.; Hiernaux, P.; Rasmussen, K.; Mbow, C.; Kergoat, L.; Tagesson, T.; Fensholt, R. Assessing woody vegetation trends in Sahelian drylands using MODIS based seasonal metrics. *Remote Sens. Environ.* **2016**, *183*, 215–225. [[CrossRef](#)]
26. Malakar, N.; Hulley, G.C. A water vapor scaling model for improved land surface temperature and emissivity separation of MODIS thermal infrared data. *Remote Sens. Environ.* **2016**, *182*, 252–264. [[CrossRef](#)]
27. Coll, C.; Garcia-Santos, V.; Niclos, R.; Caselles, V. Test of the MODIS land surface temperature and emissivity separation algorithm with ground measurements over a rice paddy. *IEEE Trans. Geosci. Remote Sens.* **2016**, *54*, 3061–3069. [[CrossRef](#)]
28. Hulley, G.C.; Hughes, C.G.; Hook, S.J. Quantifying uncertainties in land surface temperature and emissivity retrievals from ASTER and MODIS thermal infrared data. *J. Geophys. Res. Atmos.* **2012**, *117*, D23113. [[CrossRef](#)]
29. Waseem, M.; Ajmal, M.; Kim, T.-W. Development of a new composite drought index for multivariate drought assessment. *J. Hydrol.* **2015**, *527*, 30–37. [[CrossRef](#)]
30. Van Rossum, G.; Drake, F.L. *Python 3 Reference Manual*; CreateSpace: Scotts Valley, CA, USA, 2009.
31. Food and Agriculture Organization of the United Nations. *FAOSTAT Statistical Database*; FAO: Rome, Italy, 1997; Available online: <https://www.fao.org/faostat/en/#data> (accessed on 11 August 2022).

Disclaimer/Publisher’s Note: The statements, opinions and data contained in all publications are solely those of the individual author(s) and contributor(s) and not of MDPI and/or the editor(s). MDPI and/or the editor(s) disclaim responsibility for any injury to people or property resulting from any ideas, methods, instructions or products referred to in the content.